

**D. A. Malyshkin, A. Yu. Novikov, D. S. Tsvetkov**

*Institute of Natural Sciences and Mathematics,  
 Ural Federal University,  
 19 Mira St., 620002, Ekaterinburg,  
 Russian Federation  
 e-mail: Dmitry.Malyshkin@urfu.ru*

## Oxygen content and defect structure of the perovskite $\text{La}_{0.5}\text{Ba}_{0.5}\text{CoO}_{3-\delta}$

Perovskite-type complex oxide  $\text{La}_{0.5}\text{Ba}_{0.5}\text{CoO}_{3-\delta}$ , promising cathode material for solid oxide fuel cells and precursor for synthesis of double perovskite  $\text{LaBaCo}_2\text{O}_{6-\delta}$ , was prepared as a single-phase material. Its oxygen content was measured by two independent techniques in the temperature range 1000–1100 °C and at oxygen partial pressures corresponding to the stability field of cubic phase. The defect chemistry of this material was studied using the measured  $\delta = f(p\text{O}_2, T)$  dependences. The defect structure model based on the localized nature of the electronic defects was proposed and successfully verified.

**Keywords:** oxygen nonstoichiometry, perovskite, defect structure, coulometric titration.

Received: 28.06.2018. Accepted: 25.07.2018. Published: 30.07.2018.

© Malyshkin D. A., Novikov A. Yu., Tsvetkov D. S., 2018

### Introduction

The perovskite-type oxide  $\text{La}_{0.5}\text{Ba}_{0.5}\text{CoO}_{3-\delta}$  was first prepared in 1979 [1, 2]. By a number of techniques it was shown to have cubic crystal structure with  $Pm\bar{3}m$  space group (S. G.), at least when synthesized in air atmosphere with oxygen partial pressure,  $p\text{O}_2, \geq 0.21$  atm [3–17].

Depending on the synthesis method, the final annealing temperature,  $T$ , reported in the literature, varies within the fairly wide limits – from 750 [18] to 1300 °C [2]. However, the samples of  $\text{La}_{0.5}\text{Ba}_{0.5}\text{CoO}_{3-\delta}$  obtained at  $T \leq 850$  °C are usually found to contain some impurities [8, 18, 19]. Hence, regardless of the synthesis method, a single-phase cubic perovskite  $\text{La}_{0.5}\text{Ba}_{0.5}\text{CoO}_{3-\delta}$  can be prepared only at temperatures above 850 °C in air [16].

According to the results of in situ high-temperature X-ray diffraction studies [14], the crystal structure of  $\text{La}_{0.5}\text{Ba}_{0.5}\text{CoO}_{3-\delta}$  remains cubic (S. G.  $Pm\bar{3}m$ ) in the temperature range 300–800 °C and under different gas atmospheres ( $\text{O}_2$ , air and  $\text{N}_2$ ).

On the other hand, annealing of  $\text{La}_{0.5}\text{Ba}_{0.5}\text{CoO}_{3-\delta}$  at 900–1200 °C under reducing conditions led to the formation of the double perovskite  $\text{LaBaCo}_2\text{O}_{6-\delta}$  [3, 5, 10–15, 20–23]. Thus, according to the results of studying the ordering-disordering phenomenon in  $\text{LaBaCo}_2\text{O}_{6-\delta}$  –  $\text{La}_{0.5}\text{Ba}_{0.5}\text{CoO}_{3-\delta}$  system [23], the stability field of cubic perovskite at 1000–1100 °C corresponds to the  $p\text{O}_2$  range  $-1.3 \leq \log(p\text{O}_2/\text{atm}) \leq -0.68$ .

The oxygen content in the  $\text{La}_{0.5}\text{Ba}_{0.5}\text{CoO}_{3-\delta}$  was measured as a function of  $p\text{O}_2$  and temperature using coulometric titration [24] and thermogravimetric technique [6, 7, 11, 12, 14, 17]. However, the results obtained are discrepant, as evidenced by the comparison in Table 1 and in Fig. 1. Moreover, sometimes even the data reported by the same scientific group [6, 7] turn out to be inconsistent with each other, as seen in Fig. 1. Unfortunately, in most cases it is difficult

to understand the origin of these discrepancies because of the incomplete and often only superficial description of the specific experimental conditions (heating/cooling rate, equilibration time etc.) used by different authors.

The only available attempt to describe the defect structure of  $\text{La}_{0.5}\text{Ba}_{0.5}\text{CoO}_{3-\delta}$  reported in [17] should also be considered as unsuccessful due to obvious errors in the charge neutrality and mass balance conditions given in [17].

Table 1

Comparison of the available literature data on the absolute oxygen content in  $\text{La}_{0.5}\text{Ba}_{0.5}\text{CoO}_{3-\delta}$  at room temperature

The oxygen content in sample at room temperature, $3-\delta$	Cooling rate, °C/h		
	60	300	unknown
	$p\text{O}_2$ , atm		
	0.21		1
3.00	[7] <sup>2</sup>		[6] <sup>2</sup>
2.98			[14] <sup>1</sup> , [17] <sup>2</sup>
2.96			[11] <sup>2</sup>
2.94			[17] <sup>2</sup>
2.91		[12] <sup>1</sup>	

method for determining the absolute value of  $\delta$ :

<sup>1</sup> – reduction by hydrogen flux

<sup>2</sup> – iodometric titrations

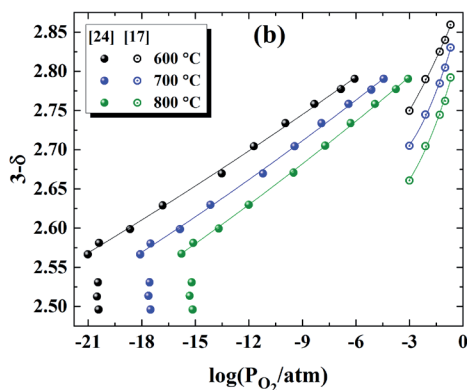
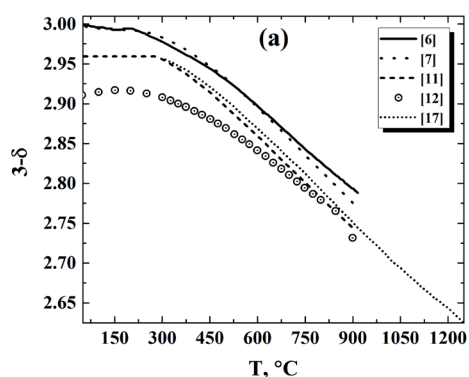


Fig. 1. a) The oxygen content in  $\text{La}_{0.5}\text{Ba}_{0.5}\text{CoO}_{3-\delta}$  as a function of temperature in air; b) The oxygen content in  $\text{La}_{0.5}\text{Ba}_{0.5}\text{CoO}_{3-\delta}$  vs.  $p\text{O}_2$  at different temperatures. The curves are shown as guides to the eye only

Therefore, the priority purposes of this work were (i) to prepare single-phase  $\text{La}_{0.5}\text{Ba}_{0.5}\text{CoO}_{3-\delta}$  oxide, (ii) to get reliable da-

ta on its oxygen content as a function of  $T$  and  $p\text{O}_2$  and (iii) to carry out the analysis of the defect structure of  $\text{La}_{0.5}\text{Ba}_{0.5}\text{CoO}_{3-\delta}$ .

## Experimental

Powder sample of the  $\text{La}_{0.5}\text{Ba}_{0.5}\text{CoO}_{3-\delta}$  was prepared by means of the glycerol-nitrate method using  $\text{La}_2\text{O}_3$ ,  $\text{BaCO}_3$  and Co as starting materials. All of the materials used had a purity of 99.99%. A stoichiometric mixture of the starting materials was dissolved in concentrated nitric acid (99.99% purity) and the required volume of glycerol (99% purity) was added as a complexing agent and a fuel. The glycerol quantity was calculated according to the amount required for the full reduction of the corresponding nitrates to molecular nitrogen  $\text{N}_2$ . The as-prepared solution was heated continuously at 100 °C until complete water evaporation and pyrolysis of the dried precursor had occurred. The resulting ash was subjected to stepwise calcination at temperatures between 900 and 1100 °C in air with intermediate regrindings. Annealing at the last stage was

carried out for 30 hours. The sample was then cooled to room temperature at a rate of 100 °C/h.

The phase composition of the powder samples prepared accordingly was studied at room temperature by means of XRD with a Shimadzu XRD 7000S diffractometer (Shimadzu, Japan) using Cu K $\alpha$  radiation. The XRD spectra showed no indication for the presence of a second phase in the as-prepared samples.

The oxygen nonstoichiometry of  $\text{La}_{0.5}\text{Ba}_{0.5}\text{CoO}_{3-\delta}$  was measured as a function of  $p\text{O}_2$  and temperature by means of thermogravimetric (TG) and coulometric titration techniques. The absolute value of  $\delta$  in  $\text{La}_{0.5}\text{Ba}_{0.5}\text{CoO}_{3-\delta}$  was determined by direct reduction of the oxide samples by hydrogen flux in the TG setup. The details can be found elsewhere [25].

## Results and discussion

The absolute oxygen content in the sample of  $\text{La}_{0.5}\text{Ba}_{0.5}\text{CoO}_{3-\delta}$  slowly (100 °C/h) cooled to room temperature was found to be  $2.992 \pm 0.005$ , in agreement with available literature data [6, 7]. The XRD pattern of the as-prepared single-phase perovskite  $\text{La}_{0.5}\text{Ba}_{0.5}\text{CoO}_{2.992}$  is shown in Fig. 2. It was indexed using the cubic  $Pm\bar{3}m$  space group. The cell parameter  $a = 3.888$  (6) Å determined as a result of the Rietveld refinement of the XRD profile (also shown in Fig. 2) is in good agreement with those reported for  $\text{La}_{0.5}\text{Ba}_{0.5}\text{CoO}_{3-\delta}$  previously [3–5, 9, 26].

The oxygen content in  $\text{La}_{0.5}\text{Ba}_{0.5}\text{CoO}_{3-\delta}$  measured as a function of  $p\text{O}_2$  and temperature is given in Fig. 3. As seen, the data

obtained by coulometric titration and TG are in good agreement with each other. It is worth noting that the presented range of  $p\text{O}_2$  corresponds to the stability field of the cubic phase as determined in [23].

For the sake of comparison, Fig. 3 also shows the results reported in Ref. [17]. It is noteworthy that the values of the oxygen content measured in the present study exceed those found in Ref. [17] on about 0.052 under the same conditions, whereas the slope of the  $p\text{O}_2$  dependences of  $3-\delta$  is practically the same in the both data sets.

In order to analyze the defect structure of  $\text{La}_{0.5}\text{Ba}_{0.5}\text{CoO}_{3-\delta}$  using the quasichemical approach,  $\text{LaCoO}_3$  with fully occupied

oxygen sublattice was chosen as a reference crystal in the same way as for related compounds [27]. In this case, the regular constituents are  $\text{La}_{\text{La}}^{\times}, \text{Co}_{\text{Co}}^{\times}$  and  $\text{O}_{\text{O}}^{\times}$ , whereas the defect species can be defined as  $\text{Ba}'_{\text{La}}, \text{V}_{\text{O}}^{\bullet\bullet}, \text{Co}'_{\text{Co}}$  and  $\text{Co}_{\text{Co}}^{\bullet}$ , where the last two point defects correspond to cobalt in the oxidation state +2 (electron localized on cobalt site) and +4 (hole localized on cobalt site), respectively.

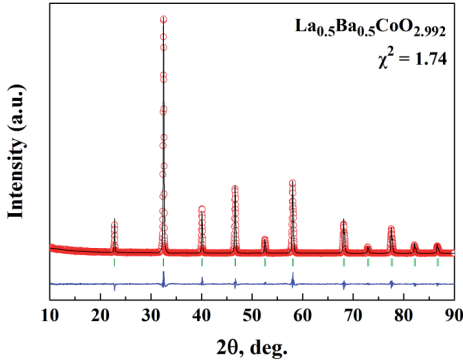


Fig. 2. Rietveld refined XRD pattern of the  $\text{La}_{0.5}\text{Ba}_{0.5}\text{CoO}_{2.992}$  sample slowly (100 °C/h) cooled from 1100 °C to room temperature in air: observed X-ray diffraction intensity (points) and calculated curve (line). The bottom curve is the difference of patterns,  $Y_{\text{obs}} - Y_{\text{cal}}$ , and the small bars indicate the angular positions of the allowed Bragg reflections

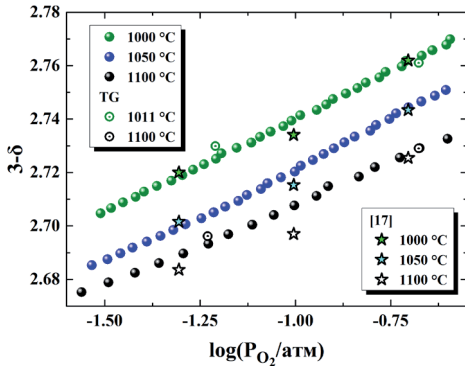
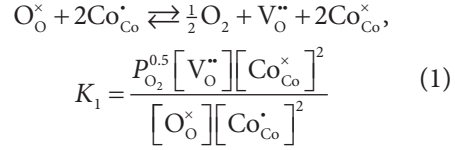
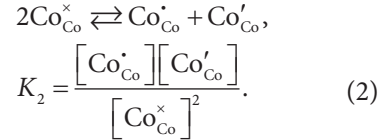


Fig. 3. Oxygen content in  $\text{La}_{0.5}\text{Ba}_{0.5}\text{CoO}_{3-\delta}$  vs.  $p\text{O}_2$  at different temperatures. Note that the data of Stingaciu [17] were shifted upward by 0.052

The following quasichemical reactions were taken into account: oxygen exchange with ambient gas atmosphere with simultaneous reduction/oxidation of cobalt (1)



and the charge disproportionation involving the transfer of an electron between adjacent sites (2)



Equilibrium constants of the proposed quasichemical reactions along with conditions of mass balance and electroneutrality form the following set of nonlinear equations:

$$\left\{ \begin{array}{l} K_1 = \frac{P_{\text{O}_2}^{0.5} [\text{V}_{\text{O}}^{\bullet\bullet}] [\text{Co}_{\text{Co}}^{\times}]^2}{[\text{O}_{\text{O}}^{\times}] [\text{Co}_{\text{Co}}^{\bullet}]^2} = \exp\left(-\frac{\Delta H_1^0}{RT} + \frac{\Delta S_1^0}{R}\right) \\ K_2 = \frac{[\text{Co}'_{\text{Co}}] [\text{Co}_{\text{Co}}^{\bullet}]}{[\text{Co}_{\text{Co}}^{\times}]^2} = \exp\left(-\frac{\Delta H_2^0}{RT} + \frac{\Delta S_2^0}{R}\right) \\ [\text{Co}'_{\text{Co}}] + [\text{Ba}'_{\text{La}}] = [\text{Co}_{\text{Co}}^{\bullet}] + 2[\text{V}_{\text{O}}^{\bullet\bullet}] \\ [\text{Co}_{\text{Co}}^{\times}] + [\text{Co}'_{\text{Co}}] + [\text{Co}_{\text{Co}}^{\bullet}] = 1 \\ [\text{O}_{\text{O}}^{\times}] = 3 - \delta \\ [\text{V}_{\text{O}}^{\bullet\bullet}] = \delta \end{array} \right. \quad (3)$$

The analytical solution of the set (3) yields the model function:

$$P_{\text{O}_2}^{0.25} = \sqrt{K_1 \frac{3 - \delta}{\delta}} \cdot \frac{12K_2 + 4\delta - 16\delta K_2 - A - 1}{2(A - 2)}, \quad (4)$$

where

$$A = \sqrt{16\delta^2 + 32\delta K_2 + 12K_2 - 64\delta^2 K_2 - 8\delta}. \quad (5)$$

Note that defect formation enthalpies were treated as constants, since the oxygen nonstoichiometry of  $\text{La}_{0.5}\text{Ba}_{0.5}\text{CoO}_{3-\delta}$  was measured in the relatively narrow temperature range. This assumption enabled the substitution of the equilibrium constants in the Eq. 4 by their thermodynamic temperature dependences (see Eq. 3) and, as a consequence, simultaneous treatment of the data on oxygen nonstoichiometry obtained at different temperatures according to the proposed defect structure model. The result of the least square fit of the model Eq. 4 to the experimental data on the oxygen content in  $\text{La}_{0.5}\text{Ba}_{0.5}\text{CoO}_{3-\delta}$  is shown in Fig. 4. As seen, there is a good agreement between the fitted surface and the measured values. The fitted parameters of the model are summarized in Table 2.

It is worth noting that the standard entropy of charge disproportionation  $\Delta S_2^0$ , obtained as a result of the least square fit, was close to zero with relatively large error margin. Within this margin fit results were found to be relatively insensitive to the particular value of  $\Delta S_2^0$ . Furthermore, it is known that the value of  $\Delta S_i^0$  corre-

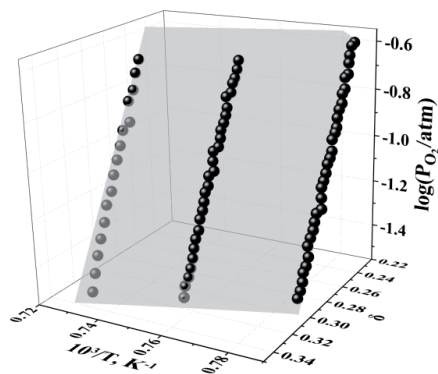


Fig. 4. The result of the least square fit of the defect structure model for  $\text{La}_{0.5}\text{Ba}_{0.5}\text{CoO}_{3-\delta}$ . Points – experimental data on oxygen nonstoichiometry of  $\text{La}_{0.5}\text{Ba}_{0.5}\text{CoO}_{3-\delta}$ . Surface – model Eq. 4 fitted

sponds to the vibrational entropy change [28] which should be very small for reaction (2) since it does not involve the gaseous species. In addition, the average point defects' coordination environment also does not change significantly in the course of the reaction (2). As a result, the magnitude of  $\Delta S_2^0$  can be expected to be rather low. Therefore, during the final fitting procedure the standard entropy of charge disproportionation,  $\Delta S_2^0$ , was assumed to be zero. Similar reasoning was also presented in Ref. [29].

Table 2  
The result of the least square fit of the defect structure model for  $\text{La}_{0.5}\text{Ba}_{0.5}\text{CoO}_{3-\delta}$

Defect reaction	$\Delta H_i^0$ , kJ·mol <sup>-1</sup>	$\Delta S_i^0$ , J·K <sup>-1</sup> ·mol <sup>-1</sup>	$R^2$
$\text{O}_\text{O}^\times + 2\text{Co}_{\text{Co}}^{\bullet\bullet} \rightleftharpoons \frac{1}{2}\text{O}_2 + \text{V}_\text{O}^{\bullet\bullet} + 2\text{Co}_{\text{Co}}^\times$	$50.9 \pm 2.1$	$35.4 \pm 1.8$	0.973
$2\text{Co}_{\text{Co}}^\times \rightleftharpoons \text{Co}_{\text{Co}}^\bullet + \text{Co}'_{\text{Co}}$	$30.1 \pm 0.5$	0.0	

## Conclusions

Oxygen nonstoichiometry of the perovskite oxide  $\text{La}_{0.5}\text{Ba}_{0.5}\text{CoO}_{3-\delta}$  was measured as a function of  $p\text{O}_2$  and tempera-

ture in the range 1000–1100 °C by means of thermogravimetric and coulometric titration techniques. The defect structure

model of  $\text{La}_{0.5}\text{Ba}_{0.5}\text{CoO}_{3-\delta}$  based on the localized nature of the electronic defects was proposed and successfully verified using the measured  $\delta = f(p\text{O}_2, T)$  dependences.

## References

1. Kobussen AGC, Van Buren FR, Van den Belt TGM, Van Wees HJA. Oxygen evolution on  $\text{LaCoO}_3$ -type electrodes. *J Electroanal Chem Interfacial Electrochem.* 1979;96(1):123–5. DOI:10.1016/S0022-0728(79)80309-5.
2. Patil SB, Keer HV, Chakrabarty DK. Structural, electrical, and magnetic properties in the system  $\text{Ba}_x\text{La}_{1-x}\text{CoO}_3$ . *Phys Status Solidi A.* 1979;52(2):681–6. DOI:10.1002/pssa.2210520240.
3. Nakajima T, Ichihara M, Ueda Y. New A-site ordered perovskite cobaltite  $\text{LaBaCo}_2\text{O}_6$ : synthesis, structure, physical property and cation order – disorder effect. *J Phys Soc Japan.* 2005;74(5):1572–7. DOI:10.1143/JPSJ.74.1572.
4. Kundu AK, Rautama EL, Boullay P, Caignaert V, Pralong V, Raveau B. Spin-locking effect in the nanoscale ordered perovskite cobaltite  $\text{LaBaCo}_2\text{O}_6$ . *Phys Rev B.* 2007;76(18):184432–1–4. DOI:10.1103/PhysRevB.76.184432.
5. Rautama E-L, Boullay P, Kundu AK, Caignaert V, Pralong V, Karppinen M, et al. Cationic ordering and microstructural effects in the ferromagnetic perovskite  $\text{La}_{0.5}\text{Ba}_{0.5}\text{CoO}_3$ : impact upon magnetotransport properties. *Chem Mater.* 2008;20(8):2742–50. DOI:10.1021/cm703314p.
6. Kim J-H, Manthiram A.  $\text{LnBaCo}_2\text{O}_{5+\delta}$  oxides as cathodes for Intermediate-Temperature Solid Oxide Fuel Cells. *J Electrochem Soc.* 2008;155(4):B385–90. DOI:10.1149/1.2839028.
7. Kim J-H, Mogni L, Prado F, Caneiro A, Alonso JA, Manthiram A. High temperature crystal chemistry and oxygen permeation properties of the mixed ionic – electronic conductors  $\text{LnBaCo}_2\text{O}_{5+\delta}$  (Ln = Lanthanide). *J Electrochem Soc.* 2009;156(12):B1376–82. DOI:10.1149/1.3231501.
8. Chen T, Zhao H, Xu N, Li Y, Lu X, Ding W, et al. Synthesis and oxygen permeation properties of a  $\text{Ce}_{0.8}\text{Sm}_{0.2}\text{O}_{2-\delta}$  –  $\text{LaBaCo}_2\text{O}_{5+\delta}$  dual-phase composite membrane. *J Membrane Sci.* 2011;370(1):158–65. DOI:10.1016/j.memsci.2011.01.007.
9. Troyanchuk IO, Karpinsky DV, Bushinsky MV, Sikolenko V, Efimov V, Cervellino A. The low-temperature macroscopic phase separation in  $\text{La}_{0.5}\text{Ba}_{0.5}\text{CoO}_{3-\delta}$  cobaltite. *JETP Letters.* 2011;93(3):139–43. DOI:10.1134/s0021364011030167.
10. Pang S, Jiang X, Li X, Su Z, Xu H, Xu Q, et al. Characterization of cation-ordered perovskite oxide  $\text{LaBaCo}_2\text{O}_{5+\delta}$  as cathode of intermediate-temperature solid oxide fuel cells. *Int J Hydrogen Energ.* 2012;37(8):6836–43. DOI:10.1016/j.ijhydene.2012.01.056.
11. Pang SL, Jiang XN, Li XN, Wang Q, Zhang QY. Structural stability and high-temperature electrical properties of cation-ordered/disordered perovskite  $\text{LaBaCoO}$ . *Mater Chem Phys.* 2012;131(3):642–6. DOI:10.1016/j.matchemphys.2011.10.029.
12. Garcés D, Setevich CF, Caneiro A, Cuello GJ, Mogni L. Effect of cationic order-disorder on the transport properties of  $\text{LaBaCo}_2\text{O}_{6-\delta}$  and  $\text{La}_{0.5}\text{Ba}_{0.5}\text{CoO}_{3-\delta}$  perovskites. *J Appl Crystallogr.* 2014;47(1):325–34. DOI:10.1107/S1600576713031233.



13. Garcés D, Mogni LV. The soft chemical route improving IT-SOFC cathode performance: The lanthanum barium cobaltite case. *ECS Trans.* 2013;58(2):191–8. DOI:10.1149/05802.0191ecst.
14. Bernuy-Lopez C, Høydalsvik K, Einarsrud M-A, Grande T. Effect of A-Site cation ordering on chemical stability, oxygen stoichiometry and electrical conductivity in layered  $\text{LaBaCo}_2\text{O}_{5+\delta}$  double perovskite. *Materials.* 2016;9(3):154–1–18. DOI:10.3390/ma9030154.
15. Garcés D, Soldati AL, Troiani H, Montenegro-Hernández A, Caneiro A, Mogni LV. La/Ba-based cobaltites as IT-SOFC cathodes: a discussion about the effect of crystal structure and microstructure on the  $\text{O}_2$ -reduction reaction. *Electrochim Acta.* 2016;215:637–46. DOI:10.1016/j.electacta.2016.08.132.
16. Setevich C, Prado F, Caneiro A. Study of the electrode polarization resistance of cobaltites with high Ba content as cathode for IT-SOFC. *J Electrochem Soc.* 2017;164(7):F759–67. DOI:10.1149/2.0681707jes.
17. Stingaciu M. Synthesis, crystal growth and investigation of layered cobaltites type  $\text{RBaCo}_2\text{O}_{5+\delta}$ . Braunschweig: Braunschweig Univ. of Technology; 2009. 114 p.
18. Zhang C, He H, Wang N, Chen H, Kong D. Visible-light sensitive  $\text{La}_{1-x}\text{Ba}_x\text{CoO}_3$  photocatalyst for malachite green degradation. *Ceram Int.* 2013;39(4):3685–9. DOI:10.1016/j.ceramint.2012.10.200.
19. Chen T, Zhao H, Xie Z, Xu N, Lu Y. Oxygen permeability of  $\text{Ce}_{0.8}\text{Sm}_{0.2}\text{O}_{2-\delta}$  –  $\text{LnBaCo}_2\text{O}_{5+\delta}$  (Ln=La, Nd, Sm, and Y) dual-phase ceramic membranes. *Ionics.* 2015;21(6):1683–92. DOI:10.1007/s11581-014-1327-5.
20. Rautama EL, Caignaert V, Boullay P, Kundu AK, Pralong V, Karppinen M, et al. New member of the “112” family,  $\text{LaBaCo}_2\text{O}_{5.5}$ : synthesis, structure, and magnetism. *Chem Mater.* 2009;21(1):102–9. DOI:10.1021/cm8021775.
21. Seddon J, Suard E, Hayward MA. Topotactic reduction of  $\text{YBaCo}_2\text{O}_5$  and  $\text{LaBaCo}_2\text{O}_5$ ; square-planar Co (I) in an Extended Oxide. *J Am Chem Soc.* 2010;132(8):2802–10. DOI:10.1021/ja910103d.
22. Hu Y, Lei J, He J, Li Y, Wang Z, Wang Y, et al. Ferromagnetic and photocatalytic properties of layered perovskite  $\text{LaBaCo}_2\text{O}_6$  nanostructures. *J Nanosci Nanotechnol.* 2016;16(1):930–3. DOI:10.1166/jnn.2016.10808.
23. Malyshkin DA, Novikov AY, Sereda VV, Ivanov IL, Tsvetkov DS, Zuev AY. In situ and ex situ study of cubic  $\text{La}_{0.5}\text{Ba}_{0.5}\text{CoO}_{3-\delta}$  to double perovskite  $\text{LaBaCo}_2\text{O}_{6-\delta}$  transition and formation of domain textured phases with fast oxygen exchange capability. Forthcoming.
24. Bernuy-Lopez C, Rioja-Monllor L, Nakamura T, Ricote S, O’Hayre R, Amezawa K, et al. Effect of Cation Ordering on the Performance and Chemical Stability of Layered Double Perovskite Cathodes. *Materials.* 2018;11(2):196. DOI:10.3390/ma11020196
25. Zuev AY, Tsvetkov DS. Conventional methods for measurements of chemo-mechanical coupling. In: Bishop SR, Perry N, Marrocchelli D, Sheldon B, editors. *Electro-chemo-mechanics of solids*: Springer International Publishing; 2017. p. 5–35. DOI:10.1007/978-3-319-51407-9

26. Suard E, Fauth F, Caignaert V. Rhombohedral distortion in the new disordered  $\text{LaBaCo}_2\text{O}_6$  perovskite. *Phys B Condensed Matter*. 2000;276–278:254–5. DOI:10.1016/S0921–4526(99)01437–4
27. Zuev AY, Petrov AN, Vylkov AI, Tsvetkov DS. Oxygen nonstoichiometry and defect structure of undoped and doped lanthanum cobaltites. *J Mater Sci*. 2007;42(6):1901–8. DOI:10.1007/s10853-006-0345-8
28. Kofstad P. Nonstoichiometry, diffusion, and electrical conductivity in binary metal oxides. New York: Wiley-Interscience; 1972. 382 p.
29. Lee Y-L, Morgan D. Ab initio and empirical defect modeling of  $\text{LaMnO}_{3+\delta}$  for solid oxide fuel cell cathodes. *Phys Chem Chem Phys*. 2012;14(1):290–302. DOI:10.1039/C1CP22380A